Search for multiple $K+L$ photoionization in solid transition elements by x-ray-absorption spectroscopy

A. Kodre, M. Hribar, I. Arčon, D. Glavič-Cindro, and M. Štuhec
J. Stefan Institute, University of Ljubljana, 61111 Ljubljana, Slovenia

R. Frahm and W. Drube
Hamburger Synchrotronstrahlungslabor HASYLAB at Deutsches Elektronensynchrotron DESY, 2000 Hamburg 52, Federal Republic of Germany

(Received 22 July 1991)

The x-ray absorption of transition metals from Cr to Zn is examined in the energy region of $K+L$ double photoabsorption. A variational procedure is developed to extract correlated components from pairs of spectra. Applied to absorption spectra taken at different sample temperatures, the procedure is used to suppress the extended x-ray-absorption fine-structure oscillations that pervade the $K+L$ region in this range of elements. A relative sensitivity of 2×10^{-3} to 3×10^{-4} of the absorption coefficient, depending on the sample quality, is achieved. No significant features attributable to multiple photoexcitation are found in the spectra on that level, so that previous reports of $K+L$ edges for Co, Ni, and Zn are not confirmed.

PACS number(s): 32.30.Rj, 32.80.Fb, 78.70.Dm

I. INTRODUCTION

Due to interelectron forces, more than one electron in an atom can be promoted to a higher orbital by absorption of a photon. Excitations of outer electrons, accompanying the inner-shell photoeffect, are fairly common, amounting up to a few tenths of the total photoabsorption cross section.

In contrast, multiple photoexcitation in inner shells is a much weaker process. Early evidence was provided by satellite lines of x-ray fluorescence spectra [1,2], produced by x-ray bombardment at photon energies high above the threshold for the process. In absorption spectroscopy, conversely, only the threshold behavior of the multiple-excitation probability can be studied: few reliable experimental results have been published so far [3–6], all of which are from absorption measurements on gaseous targets. There exist, however, a number of earlier reports of multiple-absorption edges in solid targets, including $K+L$ edges of Zn, Ge, Se, Ni, and Co [7–11], $L+L$ edges of some lanthanides [12–14], and even a $K+K$ edge of copper [15]. These data cannot be entirely reconciled with theoretical predictions, and the issue is obscured by some unclarified experimental details.

We performed a careful x-ray-absorption study of the expected $K+L$ excitation region for elements from chromium to zinc at the HASYLAB synchrotron radiation facility in Hamburg. The sensitivity of the experiments, as judged from the observed extended x-ray-absorption fine structure (EXAFS) in that region of the absorption spectra and from a study of the K-M absorption region of argon, was superior to that of the previous reports. By comparing corresponding spectra measured at room temperature and at about 80 K where the EXAFS amplitudes are considerably enhanced, it was possible to remove most of the EXAFS oscillations in the tentative $K+L$ absorption region using a numerical procedure described below. In the remaining spectrum no evidence of multiple-absorption structures was found, in contrast to the results of earlier reports where the influence of EXAFS on the data was not considered to be important. The case of Co and Ni is particularly interesting in that respect, and a detailed report has been published elsewhere [16]. For all the investigated elements the upper limits of multiple-absorption edge jumps were estimated on the basis of the experimental noise or the residual EXAFS amplitude.

II. THEORETICAL CONSIDERATIONS

Present understanding of the multiple photoexcitation process stems mainly from the work on $K+M$ photoabsorption on argon [17–19] where x-ray-absorption data have been successfully complemented by theoretical calculation and studies of fluorescence and Auger-electron spectra.

In absorption, three principal types of spectral features can be recognized according to the final state of the process. Excitation resonances and absorption edges, corresponding to neutral and singly ionized atoms in the final state, respectively, have already been known from single-electron photoabsorption spectra. Double photoionization, however, is revealed by a mere change in the slope of the cross section at threshold, following the slow rise of the accessible phase space for the two ejected electrons with excess energy. The asymptotic value of the cross section for this channel is attained only within the validity of the sudden approximation, i.e., on the order of the binding energy of the shaken electron above threshold. The effect has been demonstrated by Armen *et al.* [19] in Auger satellite spectra following $K+M$ absorption in argon. In absorption spectra double-ionization channels

have only been recognized in the shakeup and shakeoff of outermost electrons, as within the $K+M$ structure of argon [17] and at the $1s3d$ edge of krypton [20,21]. For a shakeoff from any of the deeper shells, the rise of the cross section is extended over hundreds of eV. Schaphorst *et al.* [22] showed recently that a procedure equivalent to comparison of absolute cross sections with theoretical results is necessary to reveal its presence.

So far, in experiments on multiple inner-shell photoabsorption of solid targets only relative changes of cross sections were monitored, limiting the search to the excitation resonances and single-ionization (shakeup) edges. Classification of tentative multiple-absorption edges by a simple additive scheme like $K+L_1$, L_2+L_3, etc. was based on estimates of double-ionization energies. The procedure may be misleading even when the energy difference between shakeup and shakeoff thresholds, of the order of 10 eV, is taken into account. The coupling of angular momenta in double-vacancy states can expand significantly the additive scheme. In transition elements, with their open-shell configurations, high multiplicity of final states spreads multiple-absorption thresholds into a number of small subedges, extending over tens of eV, as shown in Fig. 1 for the case of Ni[$1s,2p$]. Precise theoretical energies, possibly together with transition rate estimates, would be required for interpretation of experimental data.

Recently, another pronounced effect of state coupling has been demonstrated in multiple-photoabsorption spectra [23]. The relativistic Breit-Coulomb interaction, the current-current part of the interelectron force, exhibits a strong splitting of ns-n''s hole states. Even in argon, the singlet and the triplet $1s2s$ hole states are separated by 18 eV, one third of the $L_1-L_{2,3}$ difference. Thus at least four $K+L$ edges should be expected instead of the simple KL_1, KL_2, KL_3 triad, found in most of the mentioned reports.

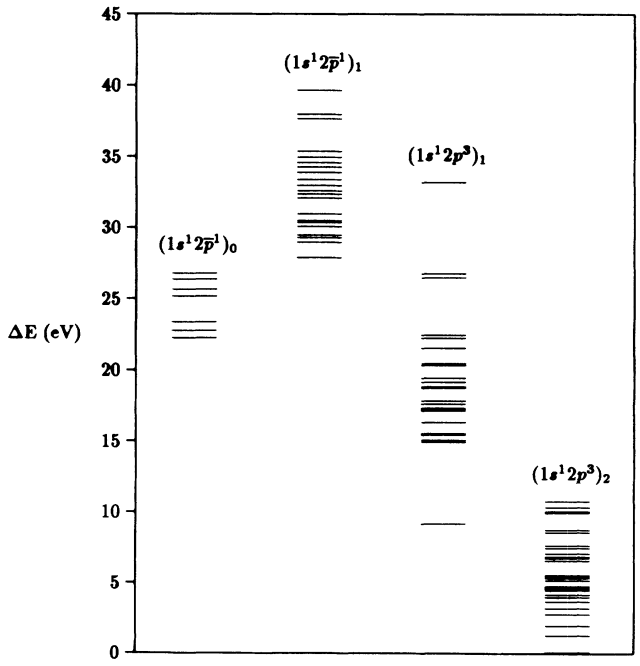

FIG. 1. Double-ionization states Ni[$1s,2p$] calculated by MCDF code [25]. The four groups of states reflect the coupling of $2p$ electrons: $(1s^12\bar{p}^1)_0$, $(1s^12\bar{p}^1)_1$, $(1s^12p^3)_1$, $(1s^12p^3)_2$. The rich splitting within groups is a consequence of the partly occupied $3d$ shell. The whole interval of final states extends over 40 eV.

III. EXPERIMENT

The experiments were performed at the EXAFS II station at HASYLAB. The synchrotron radiation from the DORIS storage ring is focused by a gold-coated mirror onto a Si(111) double-crystal monochromator with 2-eV resolution at the copper K edge. The setup with a highly stable monochromator drive is routinely used for precision x-ray-absorption spectroscopy.

Samples are inserted in a cryostat between two ionization chambers filled with nitrogen and argon, respectively, to monitor the incident and the transmitted beam. Within the integration time at each individual photon energy (typically $1s$) more than 10^9 photons are registered which is sufficient to make the statistical error of the data points negligible. For the sake of energy calibration of a wide energy region covering the K edge, the EXAFS region, and the expected $K+L$ edges region were scanned in steps of 1–5 eV. In addition, the $K+L$ region was carefully measured for a detailed search for double excitations. Hartree-Fock (HF) estimates of average $1s2s$ and $1s2p$ vacancy state energies, shown in Table I, were used to define the scan regions. By recalibration of the HF estimates to the experimental $1s$ ionization energies the large part of the systematic error of the code is taken into account. As seen from the first two columns of the table, the corrections do not exceed 20 eV. The remaining error, due to the double-vacancy interaction, is estimated to be 10 eV from a comparison of a similar HF calculation for x-ray KL satellites with data from Ref. [1].

Pure metal foils close to the optimum thickness $\mu d=2$ were used for most investigated elements (Fe–Zn). Chromium was electrodeposited onto a thin aluminum backing and manganese was prepared as a powdered sample between adhesive tapes. The absorption spectra of the metal foils were taken at room temperature and with liquid-nitrogen cooling. For some elements, powder samples of various compounds with different valence states, mostly oxides, were also used. For nickel, metallic glass foils (80 at. % Ni, 20 at. % B or P) provided spectra with particularly small EXAFS oscillations. This is due to the large static disorder in amorphous materials which gives rise to a strong damping of the EXAFS.

IV. DATA EVALUATION

The intensities of the incident and the transmitted beam, I_0 and I_{trans}, derived from the currents from both ionization chambers are stored as count rates after current-to-voltage and voltage-to-frequency conversion. Absorption spectra are conventionally presented as $\ln(I_0/I_{\text{trans}})$. The absorption thickness of the sample μd

TABLE I. Estimates of $K+L$ ionization energies (in eV): Comparison of experimental and HF values for K-shell ionization energies is used to recalibrate $K+L$ estimates from HF86 code of Froese-Fischer [24]. Reported values from previous experiments are included.

Element	$1s^1$ Expt.	$1s^1$ HF86	$1s^12s^1$ HF86	$1s^12p^5$ HF86	$1s^12s^1$ Recalibrated	$1s^12p^5$ Recalibrated	$1s^12s^1$ Prev. Experiments	$1s^12p^1_{1/2}$ Prev. Experiments
$_{24}$Cr	5989	6004	6769	6668	6754	6653		
$_{25}$Mn	6539	6553	7412	7304	7398	7290		
$_{26}$Fe	7112	7128	8058	7943	8042	7927		
$_{27}$Co	7709	7727	8740	8618	8722	8600	8655±4	8538±4 [11]
$_{28}$Ni	8332	8352	9452	9323	9472	9303	9501±3	9372±3 [10]
$_{29}$Cu	8981	8991	10170	10034	10160	10024		
$_{30}$Zn	9659	9671	10956	10816	10944	10804	10954±5	10819±5 [8]

is obtained by subtracting the analogous result of a reference experiment without sample whereby the sensitivities of the ionization chambers and the residual absorption in the target cell, such as, e.g., by the windows and adhesive tape supports, cancel out (Fig. 2). Beside random noise, some scans of I_0 reveal systematic excursions, caused by the software stabilization of the monochromator. However, both noise components divide out in μd almost completely; a small residual in some spectra can be removed numerically.

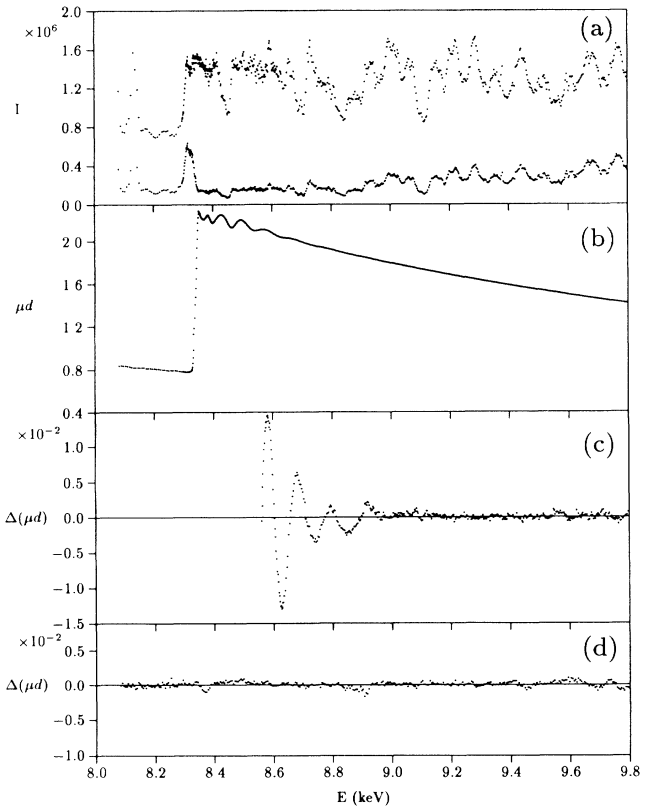

FIG. 2. Analysis of absorption spectrum of NiB glass: (a) Scans of incident beam (top) and transmitted beam (bottom). (b) Absorption $\ln(I_0/I_{\text{trans}})$. (c) Enhanced structure of μd with EXAFS after subtraction of best-fit third-order polynomial. (d) Reference spectrum without NiB sample after the same treatment as in (c).

Beyond the K edge and the EXAFS region, the spectra of μd exhibit a very smooth decrease: after subtraction of a best-fit low-order (3–5) polynomial in energy, and normalization with respect to the K-edge jump the small-scale structure of the data is enhanced. It shows that on

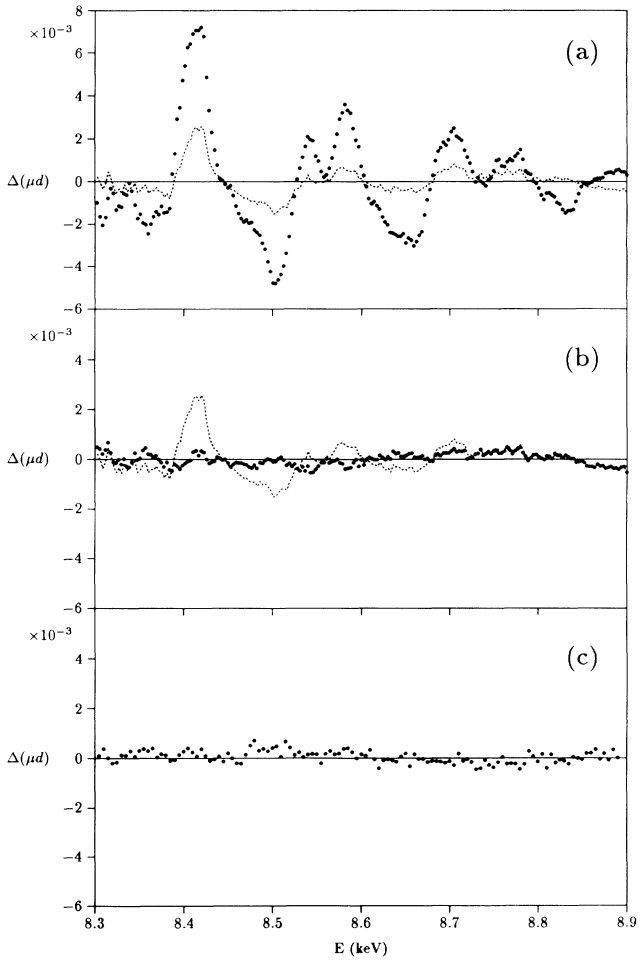

FIG. 3. Filtering out the far EXAFS structure. (a) EXAFS spectra of Co: — — —, at room temperature; · · · ·, cooled with liquid nitrogen. (b) The room-temperature spectrum (— — —) and its residual (· · · ·) after removal of EXAFS by Eq. (2). (c) The reference spectrum without cobalt sample for comparison of noise levels.

the 10^{-3} level EXAFS oscillations extend well into the $K+L$ region. The noise on that level is ascribed to the sample inhomogeneities and the noise of the detection system.

The temperature dependence of the EXAFS amplitudes, contained in the Debye-Waller factor, can be exploited to construct artificial spectra, approximating free-atom absorption. At least far beyond the K edge, away from the near-edge structure, EXAFS amplitudes are superimposed onto the atomic absorption. By cooling the sample to liquid-nitrogen temperature, the EXAFS amplitudes are increased significantly with respect to room temperature, while the atomic absorption should remain unaffected. Subtraction of the low-temperature spectrum, properly renormalized, from a corresponding high-temperature spectrum, should remove the EXAFS amplitudes, while affecting the atomic-absorption features to a smaller degree.

This intuitive notion can be operationalized in the following numerical procedure. After best-fit polynomial subtraction, whereby the leading moments of a spectral distribution are removed, the correlation coefficient

$$(F,G)=\sum_{i=1}^{N} f_i g_i$$

is a measure of similarity of two spectra F and G, with count rates f_i and g_i in the ith channel. Renormalizing the spectrum G by the factor $(F,G)/(G,G)$ is equivalent to the construction of the best fit of G onto F. Consequently, the spectrum F' with count rates

$$f_i'=f_i-g_i(F,G)/(G,G) \tag{1}$$

should be free of components common to F and G. The

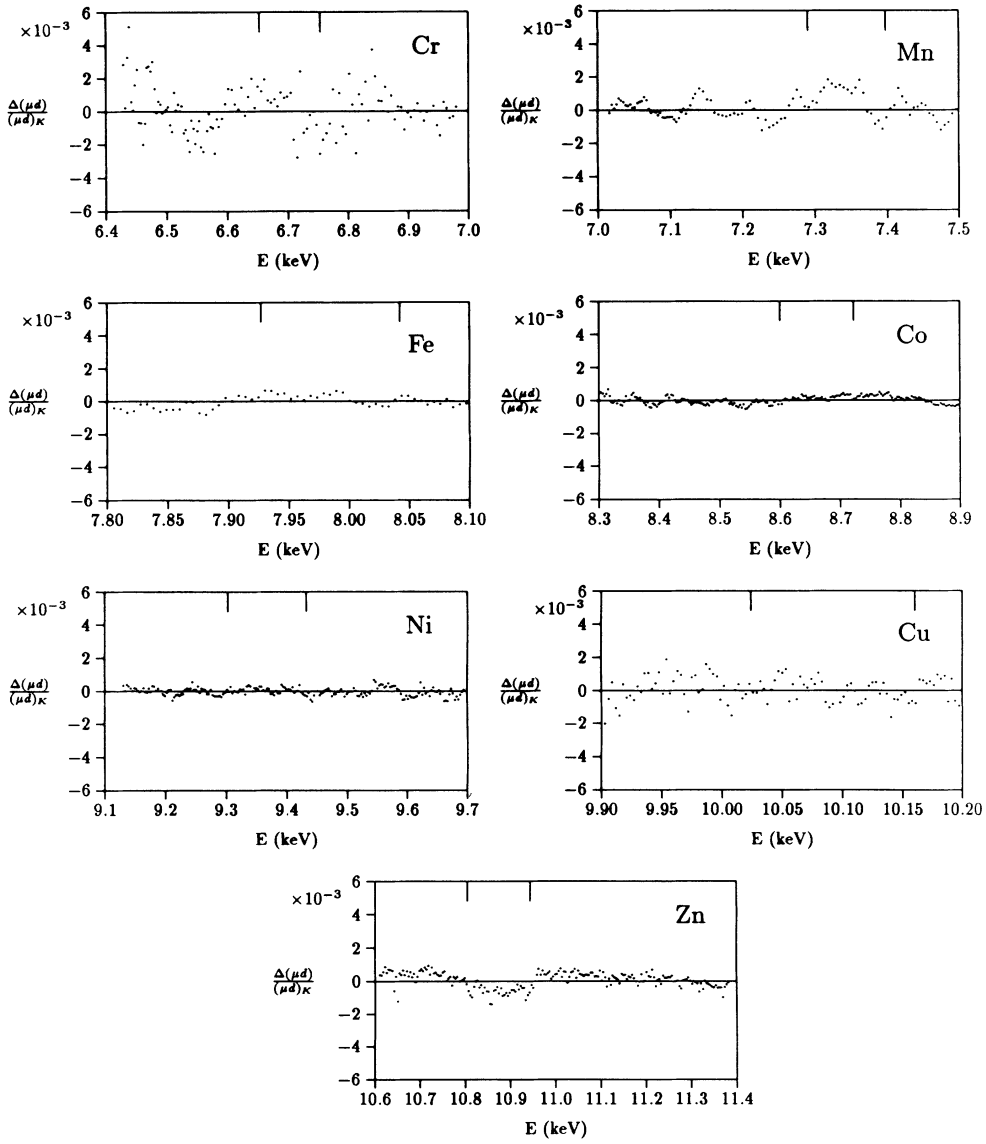

FIG. 4. Residual noise in absorption spectra of all investigated elements. Estimates of $K+L_1$ and $K+L_{2,3}$ ionization energies from Table I are indicated.

procedure is equivalent to the Gram-Schmidt orthogonalization, if spectra F and G are considered as vectors in the N-dimensional space. In our case, F is the high-temperature spectrum, and G the low-temperature spectrum serving as a template for EXAFS oscillations to be removed from F. The atomic-absorption effects in the residual F' are suppressed, with respect to F, only by the factor $1-(F,G)/(G,G)$.

In practice, an equivalent least-squares procedure is preferably adopted, with a renormalization factor α defined by a requirement that the norm of F' be minimal:

$$(F',F')=\sum_i (f_i-\alpha g_i)^2=\min\ , \tag{2}$$

whence Eq. (1) follows immediately.

Since the damping by the Debye-Waller factor depends on the wave number, the cancellation of EXAFS amplitudes by the above procedure can only be achieved within a narrow energy region. For adjacent regions, adjustments in the value of α are required. Thus the scope of the technique is expanded considerably by introducing a variable $\alpha(E_i)$ as a low-order polynomial with coefficients determined in the least-squares formulation as given in Eq. (2).

A test of the method right at the K edge shows that a complete removal of the EXAFS cannot be achieved, since the peaks in the low-temperature EXAFS are not only higher but also sharper, so that both structures are not fully similar: yet a suppression by a factor of 20 is possible and the remaining oscillations are completely out of phase with the original ones. Further out from the K edge, in the $K+L$ region, the EXAFS is sufficiently smoothed out, so that a cancellation to the level of noise is possible, as illustrated in Fig. 3 for the case of cobalt.

The same technique, with the incident-beam scan I_0 as the template vector G, is used to remove the residuals of the systematic beam noise from the I_0/I_{trans} ratio. The atomic-absorption effects in I_0/I_{trans}, absent in the I_0 scan, remain unaffected by the procedure.

V. RESULTS

With EXAFS oscillations removed from the $K+L$ region, either by using samples with strong damping of EXAFS, or by applying the numerical procedure described above, the absorption spectra exhibit a homogeneous noise at the peak-to-peak level of a few thousandths at μd values of the order of unity (Fig. 4). As expected, the noise level is lowest with metallic foil targets, due to their homogeneity, while with powder samples, the noise is typically larger by a factor of 2. The smoothest spectra, however, are obtained from materials with large static disorder, like metallic glasses. At the noise level a few features of apparently nonstochastic nature, such as peaks and steps, are found in the spectra. Steps are in both directions and either far from the estimated $K+L$ ionization energies or not reproduced in reruns: no candidates for multiple-absorption edges and excitation resonances are found.

Thus the noise levels $\delta(\mu d)$ in the processed spectra can be used as estimates for upper limits of the multiple $K+L$ absorption edge jumps. They are summarized in Table II together with energy regions considered and the corresponding K-edge jump values $\Delta(\mu d)_K$. We choose to give these limits as full noise amplitudes over a wide spectral range. This might seem excessive: indeed, edges of such amplitude would be clearly discernible. Besides, the noise amplitude could be diminished by considering a narrower energy range. Yet we feel that a safeguard against erroneous interpretation of local features close to expected edge positions is needed.

In the last two columns of Table II upper limits for

TABLE II. Experimental results: For each sample the energy region of $K+L$ edge search, K-edge jump, and residual noise level are given. Ratios of the latter two values are used as upper limits for the relative $K+L$ edge jumps and compared to previous results.

	Sample	Energy region (eV)	$\Delta(\mu d)_K$	$\delta(\mu d)_{\max}$ (units of 10^{-3})	σ_{KL}/σ_K Up. Limit (units of 10^{-3})	σ_{KL}/σ_K Prev. expt (units of 10^{-3})
Cr	depos. on Al	6 540–6 940	0.4	3.3		
	Cr_2O_3 powder	6 500–6 900	1.5	4.0		
	$K_2Cr_2O_7$ powder	6 480–6 980	1.0	2.0	2.0	
Mn	powder	7 000–7 500	1.8	2.0	1.3	
	MnO powder	7 000–7 500	3.0	4.5		
	MnO_2 powder	7 130–7 500	2.0	3.5		
	$KMnO_4$ powder	7 100–7 500	1.0	2.0		
Fe	foil 6 μm	7 800–8 200	1.9	3.0		
	Fe_2O_3 powder	7 800–8 040	3.0	6.0		
	Fe_3O_4 powder	7 800–8 100	2.5	2.0	0.8	
	$FeSO_4$ powder	7 800–8 100	0.5	1.5		
Co	foil 9 μm	8 400–8 900	2.8	1.5	0.5	2.9±0.5 [11]
Ni	foil 6 μm	9 100–9 800	1.6	0.8		
	NiP glass 19 μm	9 130–9 600	1.1	0.5		
	NiB glass 9 μm	9 140–9 600	1.5	0.4	0.3	2.5±0.4 [10]
Cu	foil 9 μm	9 900–10 200	1.7	2.0	1.3	
	$CuSO_4$ powder	9 900–10 200	0.7	1.0		
Zn	foil 12.5 μm	10 650–11 400	2.4	2.0	0.8	5.0±0.8 [8]

$K+L$ photoabsorption cross sections relative to the K-edge jump are compared to previously published results. Judging from the error bars, sensitivities of the previous experiments are comparable to ours. However, reported edges at more than fivefold noise level should, if they exist, be clearly reproduced in our spectra. The results of Salem *et al.* [8] for Zn are difficult to comment on in this view, since the data evaluation procedure, by which edges two to three times below statistical noise were extracted, is not fully reported. On the other hand, with the statistically significant results of Deutsch and co-workers [10,11] for Co and Ni metal the presence of EXAFS in the energy region of interest was not taken into account.

VI. CONCLUSIONS

The result of the present search is in agreement with theoretical predictions. In transition metals, rich multiplicity of final states in the shakeup processes smears sharp absorption features below the present experimental detection limit. We should reiterate, however, that the upper limits given in Table II only refer to the absorption edges, i.e., the shakeup contributions. They should not be compared to the total double $K+L$ cross sections from x-ray satellite data, taken far above the K edge. These include the saturated shakeoff contribution, and could, consequently be several times larger, as estimated from the extrapolation of x-ray satellite data in Ref. [1]. This is in accord with theoretical results that for deep inner-shell electrons shakeoff prevails over shakeup in the high-energy limit [26,27].

Consequently, the current accuracy of absorption spectroscopy may not be sufficient to detect multiple inner-shell photoexcitations in transition—or for that sake, most higher-Z—elements. A combination with emission studies which directly probe the excited states could prove helpful.

[1] J. Utriainen, M. Linkoaho, E. Rantavuori, T. Åberg, and G. Graeffe, Z. Naturforsch., Teil A **23**, 1178 (1968).

[2] R. D. Deslattes, Phys. Rev. **133**, A 399 (1964).

[3] M. Deutsch and M. Hart, Phys. Rev. A **34**, 5168 (1986).

[4] S. Bodeur, P. Millie, E. Lizon, I. Nenner, A. Filiponi, F. Boscherini, and S. Mobilio, Phys. Rev. A **39**, 5075 (1989).

[5] A. Kodre, S. J. Schaphorst, and B. Crasemann, in *X-Ray and Inner-Shell Processes, Knoxville,* Proceedings of the Conference on X-Ray and Inner-Shell Processes, AIP Conf. Proc. No. 215, edited by Thomas A. Carlson, Manfred O. Krause, and Steven T. Manson (AIP, New York, 1990).

[6] U. Kuetgens and J. Hormes, Phys. Rev. A **44**, 264 (1991).

[7] S. I. Salem, Brahm Dev, and P. L. Lee, Phys. Rev. A **22**, 2679 (1980).

[8] S. I. Salem, D. D. Little, A. Kumar, and P. L. Lee, Phys. Rev. A **24**, 1935 (1981).

[9] S. I. Salem, A. Kumar, and P. L. Lee, Phys. Lett. **92A**, 331 (1982).

[10] M. Deutsch and M. Hart, Phys. Rev. A **29**, 2946 (1984).

[11] M. Deutsch, M. Hart, and P. Durham, J. Phys. B **17**, L395 (1984).

[12] S. I. Salem, A. Kumar, and P. L. Lee, Phys. Rev. Lett. **25**, 2069 (192).

[13] S. I. Salem, A. Kumar, K. G. Schiessel, and P. L. Lee, Phys. Rev. A **26**, 3334 (1982).

[14] A. Kumar, B. L. Scott, and S. I. Salem, J. Phys. B **18**, 3105 (1985).

[15] S. I. Salem and A. Kumar, J. Phys. B **19**, 73 (1986).

[16] R. Frahm, W. Drube, I. Arčon, D. Glavič-Cindro, M. Hribar, and A. Kodre, in *2nd European Conference on Progress in X-Ray Synchrotron Radiation Research, Rome,* Italian Physical Society Conf. Proc. Vol. 25, edited by A. Balerna, E. Bernieri, and S. Mobilio (IPS, Bologna, 1990).

[17] R. D. Deslattes, R. E. LaVilla, P. A. Cowan, and A. Henins, Phys. Rev. A **27**, 923 (1983).

[18] R. D. Deslattes, Aust. J. Phys. **39**, 825 (1986).

[19] G. B. Armen, T. Åberg, K. R. Karim, J. C. Levin, B. Crasemann, G. S. Brown, M. H. Chen, and G. E. Ice, Phys. Rev. Lett. **54**, 182 (1985).

[20] M. Deutsch and M. Hart, Phys. Rev. Lett. **57**, 1566 (1986).

[21] E. Bernieri and E. Burattini, Phys. Rev. A **35**, 5168 (1986).

[22] S. J. Schaphorst, A. Kodre, J. Ruscheinski, B. Crasemann, M. H. Chen, J. Tulkki, T. Åberg, Y. Azuma, and G. S. Brown (unpublished).

[23] A. Kodre, S. J. Schaphorst, J. Ruscheinski, B. Crasemann, Y. Azuma, G. Brown, and M. H. Chen (unpublished).

[24] C. Froese-Fischer, Comput. Phys. Commun. **43**, 355 (1987).

[25] I. P. Grant, B. J. McKenzie, and P. H. Norrington, Comput. Phys. Commun. **21**, 207 (1980).

[26] K. G. Dyall, J. Phys. B **16**, 3137 (1983).

[27] T. A. Carlson and C. W. Nestor, Jr., Phys. Rev. A **8**, 2887 (1973).